Engrailed-2 promotes a malignant phenotype of esophageal squamous cell carcinoma through upregulating the expression of pro-oncogenic genes

Yong Cao [1] , **Xiaoyan Wang** [1] , **Li Tang** [1] , **Yan Li** [1] , **Xueqing Song** [1] , **Xu Liu** [1] , **Mingying Li** [1] , **Feng Chen** [1] , **Haisu Wan**
Corresp. 1

[1] Experimental Medicine Center, The Affiliated Hospital of Southwest Medical University, Luzhou, Sichuan, China

Corresponding Author: Haisu Wan
Email address: whssyzx@swmu.edu.cn

Background. A number of homeobox genes have been implicated in the development of various cancers. However, the role of engrailed 2 (EN2), a member of the homeobox gene superfamily, in esophageal squamous cell carcinoma (ESCC) remains unknown.

Methods. The expression of EN2 was examined using quantitative real-time PCR and immunohistochemistry. A stable cell line was established to express exogenous EN2 using a lentivirus system. The malignant phenotype was analyzed with proliferation, clonogenicity, wound-healing, and invasion assays. The CRISPR/Cas9 system was adopted to deplete endogenous EN2. RNA profiling was performed using gene expression microarray. The ShRNA-mediated method was used to knock down the expression of SPARC. The structure–function relationship was determined using site-directed mutagenesis.

Results. EN2 is highly expressed in ESCC. The malignant phenotype of the ESCC cell line was amplified by an overexpression of EN2 but was attenuated by a disruption of EN2. RNA profiling analysis revealed that distinct sets of genes were modulated by the expression of EN2 in various ESCC cell lines, and oncogenes were among these. EN2 greatly increased the expression of SPARC in Eca109. Site-directed mutagenesis revealed that the induction of SPARC was closely correlated with the protumor function of EN2. ShRNA-mediated knockdown of SPARC attenuated the malignant phenotype of EN2-infected cells. These data suggest that SPARC is crucial for mediating the protumor function of EN2.

Discussion. EN2 has an oncogenic function in ESCC that is mediated by upregulating the expression of pro-oncogenic genes downstream. EN2 may be a potentially act as a diagnostic marker or therapeutic target for ESCC treatment in the future.

1 **Engrailed-2 promotes a malignant phenotype of esophageal squamous cell carcinoma**

2 **through upregulating the expression of pro-oncogenic genes**

3 Yong Cao[1], Xiaoyan Wang[1], Li Tang[1], Yan Li[1], Xueqing Song[1], Xu Liu[1], Mingying Li[1], Feng

4 Chen[1] and Haisu Wan[1]

6 1 Experimental Medicine Center, The Affiliated Hospital of Southwest Medical University,

7 Luzhou, Sichuan, China

9 Corresponding Author:

10 Haisu Wan[1]

11 No. 25, Taiping Street, Luzhou, Sichuan, 646000, China.

12 Email address: whssyzx@swmu.edu.cn

13 **Abstract**

14 **Background.** A number of homeobox genes have been implicated in the development of various

15 cancers. However, the role of engrailed 2 (EN2), a member of the homeobox gene superfamily,

16 in esophageal squamous cell carcinoma (ESCC) remains unknown.

17 **Methods.** The expression of EN2 was examined using quantitative real-time PCR and

18 immunohistochemistry. A stable cell line was established to express exogenous EN2 using a

19 lentivirus system. The malignant phenotype was analyzed with proliferation, clonogenicity,

20 wound-healing, and invasion assays. The CRISPR/Cas9 system was adopted to deplete

21 endogenous EN2. RNA profiling was performed using gene expression microarray. The ShRNA-

22 mediated method was used to knock down the expression of SPARC. The structure–function

23 relationship was determined using site-directed mutagenesis.

24 **Results.** EN2 is highly expressed in ESCC. The malignant phenotype of the ESCC cell line was

25 amplified by an overexpression of EN2 but was attenuated by a disruption of EN2. RNA

26 profiling analysis revealed that distinct sets of genes were modulated by the expression of EN2

27 in various ESCC cell lines, and oncogenes were among these. EN2 greatly increased the

28   expression of SPARC in Eca109. Site-directed mutagenesis revealed that the induction of

29   SPARC was closely correlated with the protumor function of EN2. ShRNA-mediated

30   knockdown of SPARC attenuated the malignant phenotype of EN2-infected cells. These data

31   suggest that SPARC is crucial for mediating the protumor function of EN2.

32   **Discussion.** EN2 has an oncogenic function in ESCC that is mediated by upregulating the

33   expression of pro-oncogenic genes downstream. EN2 may potentially act as a diagnostic marker

34   or therapeutic target for ESCC treatment in the future.

35   **Introduction**

36   Esophageal squamous cell carcinoma (ESCC) is one of the most common malignancies

37   diagnosed in China and worldwide and is associated with high rates of morbidity and mortality

38   (Lin et al. 2013). The overall 5-year survival rate of ESCC patients is in the low range of 15-25%

39   (Domper Arnal et al., 2015). Significant efforts have been made to determine the molecular

40   events that occur during cancer development with the expectation that a better understanding of

41   the molecular mechanisms will help to identify more diagnostic markers or therapeutic targets

42   and may improve clinical outcomes.

43   Homeobox genes in humans are part of a superfamily with approximately 300 members. The

44   associated genes have a homeobox region, approximately 180 base pairs in length, which

45   encodes a highly conserved homeodomain (HD) with a length of about 60 amino acids

46   (Madissoon et al., 2016). The homeobox proteins are transcription factors that can activate or

47   repress the genes downstream (Carnesecchi et al., 2018). The homeodomain is responsible for

48   the sequence-specific binding of the homeobox protein to its target DNA. The three-dimensional

49   structure of the homeodomain consists of three alpha-helices connected by two short loops,

50   which form the structural basis for direct contact with DNA (Fraenkel et al., 1998; Pabo & Sauer,

51   1992). Homeobox genes are crucial for normal embryonic development and the maintenance of

52   adult cells (Friedrich et al., 2016; Hueber & Lohmann, 2008). The aberrant expression of

53   homeobox genes has been observed in a variety of cancers (Mansour & Senga, 2017; Teo et al.,

54   2016; Zhang et al., 2018).

55   Engrailed 2 is one member of the homeodomain-containing transcription factor. It is engaged in

56   the development of the nervous system at the embryonic stage and in the establishment and

57   maintenance of the spatial integrity of specific regions of developing tissues (McGrath et al.,

58   2013; Morgan, 2006). Previous studies have demonstrated that the EN2 gene is highly expressed

59   in cancers of the prostate and breast (Bose et al., 2008; Martin et al., 2005). Our study provides

60   evidence for the role of EN2 in the development of ESCC by its activation of downstream

61   oncogenic genes.

62   **Materials & Methods**

63   **Cell lines and culture**

64   The ESCC cell lines, Eca109, Kyse150, and TE-1 were obtained from the Type Culture

65   Collection of the Chinese Academy of Sciences (Shanghai, China). The immortalized human

66   esophageal epithelial cell line (HEEC) and 293FT cell lines were obtained from Shanghai

67   Tongpai Biotechnology Co. LTD (Shanghai, China). HEEC and 293FT cells were maintained in

68   Dulbecco's Modified Eagle's Medium (DMEM) (Invitrogen, Carlsbad, CA, USA) and were

69   supplemented with 10% fetal bovine serum (FBS) (Invitrogen, Carlsbad, CA, USA). The ESCC

70   cell lines were cultured in Roswell Park Memorial Institute 1640 medium containing 10% fetal

71   bovine serum. All cells were maintained at 37°C in a 5% CO_2-humidified incubator.

72   **Patients and samples**

73   We collected 32 pairs of ESCC tissues and their matched adjacent tissues from the Department

74   of Thoracic Surgery of the Affiliated Hospital of Southwest Medical University (Lu Zhou,

75   China). All patients underwent potentially curative surgery without preoperative chemotherapy

76   or radiotherapy. This study was approved by the ethics review board at the Affiliated Hospital of

77   Southwest Medical University (K2018002-R). All of the participants involved in our study

78   provided written informed consent.

79   **Total RNA extraction and RT-PCR assay**

80   Total RNA was extracted from tumor samples or cells using Trizol reagent (Invitrogen, Carlsbad,

81   CA, USA). Four hundred nanograms of total RNA from each sample were reverse-transcribed

82   into cDNA using the PrimeScript™ RT reagent kit with gDNA Eraser (Takara, Dalian, China).

83   qRT-PCR was performed using the SYBR Premix Ex Taq II Kit (Takara, Dalian, China)

84   according to the manufacturer's instructions. The specific primers used are shown in Table S1.

85   The expression of GAPDH was used as an internal control. The RNA expression levels of genes

86   were evaluated by the 2-ΔΔct method. All specimens were examined in triplicate.

87   **Construction of the lentiviral vectors and establishment of stable cell lines**

88   The plasmids pVAX-EN2 and pCDH-NEO were constructed in the laboratory and used to

89   generate the EN2-expressing vector. Human EN2 cDNA (G136030, youbio, Hunan, China) was

90   amplified and cloned into pVAX1 for pVAX-EN2 (VT1048, youbio, Hunan, China) using the

91   HindIII and XhoI sites. The copGFP sequence was replaced with the neomycin gene in the

92   plasmid pCDH-CMV-MCS-EF1-copGFP (JiRan, Shanghai, China) for pCDH-NEO. The EN2

93   cDNA was then amplified from pVAX-EN2 and subcloned into the XhaI and BamHI sites of

94   pCDH-NEO. The resultant vector was named pCDH-EN2. The ShRNA vector for the human

95   SPARC gene was created by inserting the shRNA-SPARC sequence into the BamHI and EcoRI

96   sites of pLVX-shRNA2 (JiRan, Shanghai, China). A scramble sequence was inserted into the

97   same sites to establish a control vector. All of the constructed vectors were verified by Sanger

98   sequencing.

99   The related sequences are as follows:

100   ShRNA-SPARC sense: 5'-gatcc cggcg gttgt tcttt cctca cattt caaga gaatg tgagg aaaga acaac cgttt

101   ttt-3' and antisense: 5'-aatta aaaaa cggtt gttct ttcct cacat tctct tgaat gtgag gaaag aacaa ccgcc gg-3';

102   scramble sense: 5'-gatcc cggta caaca gccac aacgt ctatt caaga gatag acgtt gtggc tgttg tattt ttt-3' and

103   antisense: 5'-aatta aaaaa tacaa cagcc acaac gtcta tctct tgata gacgt tgtgg ctgtt gtacc gg-3'.

104   The stable cell lines were established by cotransfecting 293FT cells with the correct respective

105   lentiviral vector, which was either pCDH-EN2 or pCDH-NEO (control); and the pSPAX2

106   (VT1444, youbio, Hunan, China) and pMD2.G (VT1443, youbio, Hunan, China) package

107   plasmids using PEI reagent (Polysciences, Warrington, PA, USA), following standard laboratory

108   protocol (Toledo et al. 2009). The supernatant containing the virus particles was collected after

109   three days and was used to infect the Eca109 and Kyse150 cell lines. The positive cell clones

110   were selected using G418 (500 μg/mL; Thermo Fisher Scientific, Waltham, MA USA) and were

111   named EN2-Eca109, NEO-Eca109, EN2-Kyse150, and NEO-Kyse150. To assess the function of

112   SPARC, shRNA-SPARC was lentivirally infected into either EN2-Eca109 or NEO-Eca109. The

113   positive cells were selected after 48-hours using flow cytometry based on the expression of

114   EGFP.

115   **Immunofluorescent staining**

116   Cells were incubated for monolayer growth on glass slides at 37 °C, 5% CO2 for 24 h. The cell

117   lines were removed from the culture medium and fixed in 4% paraformaldehyde for 15 minutes

118   at room temperature, followed by an overnight incubation with polyclonal goat anti-EN2

119 antibody (ab45867; Abcam, Cambridge, UK) diluted (1:100) in 1% BSA. FITC-conjugated

120 rabbit anti-goat immunoglobulin G (ZSGB-Bio, Beijing, China) was used as the secondary

121 antibody (diluted at 1:200). Cells stained with the secondary antibody were used as the negative

122 control group. Images were collected using a Leica confocal microscope (SP8; Leica, Wetzlar,

123 Germany).

124 **CRISPR construct and clone selection**

125 The DNA sequence surrounding the initial amino acid code in the EN2 locus was selected as the

126 target of this experiment following the guidelines provided on the website of the Feng Zhang

127 Laboratory (http://crispr.mit.edu/). The Cas9 targeting sequence (Cas9-EN2) was formed by

128 annealing two complementary DNA oligos, i.e., sgRNA-EN2-sense and sgRNA-EN2-antisense;

129 this sequence was cloned into the BbsI site of the PX458 vector (#48138; Addgene, Watertown,

130 MA, USA). The resultant vector, pCas9-EN2, or PX458 vector (control), was transfected into

131 TE-1 cells using Lipofectamine 3000 (Thermo Fisher Scientific, Waltham, MA USA) according

132 to the manufacturer's instructions. EGFP-positive cells were selected after 24 hours by flow

133 cytometry and were cultured in 96-well plates with a concentration of one cell per well.

134 Individual colonies were propagated after a two-week incubation period. The genomic DNA was

135 extracted and PCR-amplified using primer-1 and primer-2. The disruption of the gene was

136 further verified using the mismatch-sensitive T7 endonuclease assay (Bressan et al., 2017; Cong

137 & Zhang, 2015).

138 The sequences of the oligos and primers used in this experiment were as follows: SgRNA-EN2-

139 sense: 5'-caccg cggta gcagc ccggg cgaag-3'; sgRNA-EN2-antisense: 5'-aaacc ttcgc ccggg ctgct

140 accgc-3'; primer-1: 5'-tgtgc aaaga tccga gctgt cagag a-3'; and primer-2: 5'-aacgg gtgga caggg tctct

141 acct-3'.

142 **Site-directed mutagenesis**

143 Mutants of the human EN2 gene were generated using our own previously established protocol

144 (Wan et al., 2012). pVAX-EN2 was used as the template. The vector sequence was amplified

145 using a pair of vector primers, VP1 and VP2, which were subjected to Esp 3I digestion. The

146 digested product was self-ligated to generate the expected mutant. The vectors with the expected

147 mutations were verified using Sanger sequencing. The mutated EN2 sequences were then cloned

148 into pCDH-NEO. The vector primers and oligos used in this experiment were as follows: Mut.1-

149   VP1: 5'-aatta cgtct cagag ccaga acaag cgcgc caaga t-3'; Mut.1-VP2: 5'-aatta cgtct cagct cagct

150   cctgc gccag gc-3'; Mut.2-VP1: 5'-aattt cgtct caacg ggcaa caaga acacg ctggc-3'; and Mut.2-VP2:

151   5'-aattt cgtct caccg tgaac caaat cttga tctgt gactc gt-3'.

152   **Proliferation and colony-formation assay**

153   Cell proliferation was examined using both the Cell Counting Kit-8 assay and the live-cell

154   imaging assay. Cells were seeded into 96-well plates at concentrations of 3,000 cells/well using

155   the Cell Counting Kit-8 (CK04, Dojindo, Tokyo, Japan). The culture medium for each cell was

156   replaced at 24, 48, and 72 hours with a solution containing 100 μL of fresh medium and 10 μL of

157   CCK-8 solution; the cells were incubated at 37°C in the dark for one hour. The absorbance (A)

158   value of each well was measured at a wavelength of 450 nm. Cells were seeded in 96-well

159   culture plates for the live-cell image assay at concentrations of 3,000 cells/well and were placed

160   in the IncuCyte Live-Cell Imaging System (Essen Bioscience, Ann Arbor, MI, USA). Growth

161   curves were calculated from confluence measurements using image analysis software. Cells were

162   seeded in six-well plates for the colony formation assay at concentrations of 200 cells/well and

163   the growth medium was changed at three-day intervals. The clones were fixed with 4%

164   formaldehyde for 10 minutes and stained with freshly prepared diluted Giemsa solution for 15

165   minutes. The clones were then counted and photographed.

166   **Wound healing and matrigel invasion assay**

167   Cells were plated in 96-well plates. After the cells reached 90%–100% confluency, a wound was

168   made using the Essen Bioscience 96-pin wound maker (Essen BioScience, Ann Arbor, MI, USA),

169   which generated a cell-free space approximately 600 μm wide. The cells were washed twice with

170   PBS to remove the floating cells. 100 μL of culture medium containing 1% FBS was added to

171   the cells for a migration assay. A Matrigel invasion assay was performed in which cells were

172   covered with 50 μl of Matrigel solution containing 3 mg/mL Matrigel (Matrigel Basement

173   Membrane Matrix, 354234, BD Biosciences, San Jose, CA, USA) that was solidified after an

174   incubation period of 30 minutes at 37°C. The matrix was overlaid with an additional 100 μL of

175   normal growth medium. Wound confluency was monitored using the IncuCyte Live-Cell

176   Imaging System. A cell wound healing software module (Essen BioScience, Ann Arbor, MI,

177   USA) (Gujral et al. 2014)was used for image analysis. The wound width was used to calculate

178   the rate of migration and invasion.

179   **Gene expression profiling**

180 Total RNA was extracted using Trizol (Invitrogen, Carlsbad, CA, USA); a total of 500 ng of

181 RNA was used for cDNA synthesis. The following experiment was performed in consultation

182 with Gene Company Ltd. (Hong Kong, China). Gene expression profiles were accessed using the

183 human Affymetrix Clariom S Assay (902926). Microarrays were scanned using the GeneChip®

184 Scanner 3000 7G. The data were analyzed with the robust multichip analysis (RMA) algorithm

185 using default analysis settings and global scaling. Normalization method values were presented

186 according to log2 RMA signal intensity. R package limma (Ritchie et al., 2015) was used to

187 obtain differential expression genes (DEGs); the cutoff fold-change was set at > 1.5 or < -1.5

188 and p-value < 0.05. The DEGs were applied in Gene Ontology analysis by R package

189 ClusterProfiler (Yu et al., 2012). The transcriptomic data in this article has been uploaded to the

190 GEO repository with the accession number GSE136331.

191 **Western blot assay**

192 The total cellular protein was extracted using a pre-cooled RIPA buffer (Cell Signaling, Danvers,

193 MA, USA) with protease and phosphatase inhibitors. Protein samples were separated by SDS-

194 PAGE and then transferred to 0.45-μm PVDF membranes (Millipore, Billerica, MA, USA). The

195 membranes were soaked in a blocking solution of 5 % skim milk in Tris-buffered saline (TBS)

196 for 1 hour and incubated overnight at 4°C with a primary anti-SPARC antibody (AF941, R&D),

197 a primary antibody dilution buffer (P0023A, Beyotime) diluted to a ratio of 1:1000, and anti-β-

198 tubulin antibody (AF1216; R&D) with a 1:1000 dilution. The blots were subsequently incubated

199 with the homologous HRP-conjugated secondary antibody (Sigma-Aldrich, St. Louis, MO, USA).

200 Immunoreactive bands were detected using ECL reagents (Thermo Fisher Scientific, Waltham,

201 MA, USA).

202 **Immunohistochemistry**

203 Formalin-fixed, paraffin-embedded sections were treated with 3% H2O2 for 10 minutes after

204 routine deparaffinization in xylene and rehydration in decreasing concentrations of ethanol

205 (100%, 95%, 85%, and 75%), followed by a period of heating in citrate sodium for antigen

206 retrieval for approximately three minutes. The sections were incubated with 10% normal goat

207 serum for 20 minutes to block nonspecific reactions after antigen retrieval. The sections were

208 then incubated overnight at 4°C with mouse monoclonal antibody, diluted at 1:200, against

209 human EN2 (Santa Cruz Biotechnology, Dallas, TX, USA). After the incubation of the primary

210 antibody, the streptavidin/peroxidase amplification kit (ZSGB-Bio, Beijing, China) was used for

211   the EN2 antigen–antibody reaction. The sections were treated with diaminobenzidine to promote

212   the appearance of the EN2 signal. Two pathologists were invited to independently score the

213   immunohistochemical signals according to intensity (0–3) and positive percentage (0–100%).

214   The intensity of positive staining was scored as: 0, negative (-); 1, weak (+); 2, moderate (++);

215   and 3, strong (+++). The expression of EN2 was calculated as the product of the intensity and

216   positive percentage × 100 (IHC score).

217   **Statistical analysis**

218   SPSS version 16.0 software (IBM Corp., Armonk, NY, USA) was used for statistical analysis.

219   All experimental data are presented as the mean ± standard deviation from at least three separate

220   experiments. The significance of the mean values between the two groups was analyzed using a

221   two-tailed Student's t-test. Pearson's correlation coefficient was used to analyze the mRNA

222   expression data obtained from qRT-PCR to provide a correlation analysis of EN2 and SPARC

223   expression in the ESCC tissue samples. Statistical p-values of less than 0.05 were considered to

224   be statistically significant.

225   **Results**

226   **EN2 is highly expressed in ESCC tissues**

227   Engrailed-2 (EN2), a member of the homeobox superfamily, is highly expressed in a number of

228   cancers, including cancers of the bladder, prostate, and breast (Bose et al., 2008; Martin et al.,

229   2005; Morgan et al., 2011; Morgan et al., 2013). The function of EN2 in ESCC is currently

230   unknown and its role was evaluated to further reveal the molecular events linked to the

231   carcinogenesis of ESCC. The expression level of EN2 was first bioinformatically analyzed using

232   two individual datasets from the NCBI GEO database, including GSE130078 and GSE45670 as

233   well as on TCGA database. The mRNA expression of EN2 was found to be significantly

234   elevated in ESCC tissues (Figs. 1A -1C). Surgical specimens derived from ESCC patients were

235   used to examine the expression level of EN2 using quantitative real-time polymerase chain

236   reaction (qRT-PCR) to support these results. The mRNA expression levels of EN2 were

237   significantly upregulated in ESCC tissues compared with the paired adjacent normal tissues (p =

238   0.0005; Fig. 1D). Immunohistochemistry was used to analyze the expression of the EN2 protein

239   in tissues. The EN2 protein expression in ESCC was significantly elevated compared with the

240   adjacent normal tissues (Figs. 1E and 1F). These results confirmed that EN2 is highly expressed

241   in ESCC at both the mRNA and protein-specific levels.

242   **EN2 promotes proliferation and clonogenic abilities of ESCC cell lines**

243   Homeobox genes have emerged as key players in the development of cancer so understanding

244   the function of EN2 in ESCC is of great interest. The mRNA expression levels of EN2 were

245   examined in three ESCC cell lines, namely Eca109, Kyse150, and TE-1, as well as the SHEE

246   cell line, which is an immortalized epithelial cell line derived from the fetal esophageal

247   epithelium induced by HPV 18 E6E7 AAV (Shen et al., 2003). A normal RNA sample was

248   included as a reference, which had an equal molar ratio of total RNA samples from the 32

249   normal samples to that of the tumor samples from the 32 ESCC patients. The mRNA expression

250   of EN2 in Eca109 and Kyse150 was lower than TE-1 (Fig. 2A), and the latter two cell lines were

251   used to study the effect of exogenously expressed EN2 on ESCC cell lines. The lentiviral system

252   was adopted to introduce EN2 into the cell lines. The expression of EN2 transcripts was greatly

253   increased, as was expected (Fig. 2B). The expression of the EN2 protein was confirmed using an

254   immunofluorescence assay (Figs. 2C and 2D). The growth capacity of the EN2-infected cells

255   was evaluated and the growth rates of both EN2-Eca109 and EN2-Kyse150 were significantly

256   increased compared with those of NEO-Eca109 and NEO-Kyse150 (Fig. 2E). Cell growth was

257   also measured using the IncuCyte Zoom live-cell imaging assay, which showed that EN2

258   promoted the proliferation of the two cell lines (Fig. 2F). The effect of EN2 on the colony-

259   forming ability of Eca109 and Kyse150 was also examined and the results revealed that both

260   EN2-infected cell lines obtained the augmented capacity of colony formation, however, the

261   effect was more apparent in Eca109 (Figs. 2G-2J).

262   **EN2 facilitates migration and invasion of ESCC cell lines**

263   Cancer cells are characterized by their ability to migrate and invade other cells. We tried to

264   determine the effects of EN2 on these malignancy-associated phenotypes. The wound-healing

265   assay was used to examine the effects of EN2 on the migration of ESCC cell lines; EN2-

266   Kyse150 (Figs. 3A and 3B) and EN2-Eca109 (Figs. 3C and 3D) cells migrated faster than did

267   their respective empty controls . Their invasive ability was examined in the Matrigel using a live-

268   cell imaging assay. The results revealed that both Kyse150 (Figs. 3E and 3F) and Eca109 (Figs.

269   3G and 3H) were more aggressive in the Matrigel after the introduction of exogenous EN2.

270   These results indicate that EN2 could promote the malignant phenotypes of ESCC cells.

271 **Disruption of EN2 inhibits the proliferation, clonogenicity, migration and invasion of**
272 **ESCC cells**

273 The CRISPR/Cas9 system was used to investigate the biological function of EN2 in ESCC by
274 generating EN2 null cells in TE-1, in which EN2 is highly expressed. The CRISPR/Cas9
275 machinery was designed to destroy the gene structure of the first exon (Fig. 4A). One positive
276 clone was chosen for experimentation. The successful disruption of the EN2 gene was confirmed
277 using the mismatch-sensitive T7 endonuclease assay (Fig. 4B), in which the appearance of bands
278 of 744 bp and 354 bp indicated the expected modification of the target site in the EN2 locus. The
279 PX458 empty vector was transfected into TE-1 cells to generate a control cell line. The
280 expression of the EN2 protein was eliminated in the EN2-disrupted cells as determined by the
281 immunofluorescent staining assay (Fig. 4C). We subsequently assessed whether the disruption of
282 EN2 affects the malignant phenotype of TE-1 cells. TE-1 cells with the disrupted EN2 locus
283 exhibited a reduced growth rate (Fig. 4D). Their colony-forming ability was also weakened when
284 compared with the control (Figs. 4E and 4F). The disruption of EN2 hindered the migration (Figs.
285 4G and 4H) and invasive (Figs. 4I and 4J) behavior of TE-1 cells. These results demonstrate that
286 the disruption of EN2 negatively affects the malignant phenotype of TE-1 cells and further
287 supports its oncogenic role in ESCC.

288 **EN2 upregulates the expression of SPARC**
289 EN2 is similar to other homeodomain proteins in its ability to bind to the sequence-specific DNA
290 sites in the chromosome and consequently regulate the downstream genes like other transcription
291 factors. The genetic expression profiling in EN2-Eca109 and EN2-Kyse150 cells was analyzed
292 to determine the molecular mechanisms responsible for their protumor functions. The
293 transcriptomic data were obtained using the Affymetrix clariom S array to examine their genetic
294 expression. A total of 62 genes were found to be upregulated (Table S2) and 42 genes were
295 downregulated (Table S3) in the EN2-Eca109 cells as compared with the NEO-Eca109 cells (Fig.
296 5A). A total of 131 genes were found to be upregulated (Table S4) and 249 genes downregulated
297 (Table S5) in the EN2-Kyse150 cells compared with the NEO-Kyse150 cells (Fig. S1A)
298 Gene ontology analysis was conducted to determine the biological function of EN2-regulated
299 genes. The genes upregulated by EN2 in Eca109 are categorized into groups including cAMP-
300 dependent kinase inhibition, extracellular matrix binding, protein kinase A activity, growth

301   receptor binding, cytokine receptor activity, and phosphoric diester hydrolase activity (Fig. 5B).

302   The genes upregulated by EN2 in Kyse150 are categorized into groups including ErbB-2 class

303   receptor binding, extracellular matrix constituent, proteinaceous extracellular matrix, and

304   response to type I interferon (Fig. S1B). The results of the GO analysis of the downregulated

305   genes are shown in Figs. 5C and S1C respectively. These data suggest that EN2 is able to

306   upregulate genes connected to the malignant characteristics of ESCC cells. A segment of gene

307   expression was verified using qRT-PCR analysis (Figs. 5D and S1D). There are many well-

308   documented pro-oncogenic genes (Kojima et al., 2019; Tian et al., 2016; Wu et al., 2019) that are

309   upregulated upon the expression of EN2, implying that EN2 could modulate the expression of

310   the downstream targets genes in a cellular, context-dependent manner.

311   The upregulated oncogenic gene was investigated for its role in mediating the biological function

312   of EN2 using SPARC in the Eca109 cell line. The secreted protein acidic and rich in cysteine

313   (SPARC) is a multi-faceted protein that has a well-documented function in the malignant

314   features of various types of cancer (Chen et al., 2012; Hung et al., 2017). The mRNA level of the

315   SPARC gene increased by about 25 fold with EN2 in Eca109 cells (Fig. 5D). The protein level

316   also increased by approximately 7.5 fold, as determined by western blot testing (Fig. 5E). Our

317   results indicate a drastic induction of SPARC in EN2-Eca109, implying a possible positive

318   correlation between the expression of EN2 and SPARC. We examined both EN2 and SPARC

319   expression in the clinical ESCC samples using qRT-PCR; the results verified the positive

320   correlation of ESCC (Fig. 5F). The expression of SPARC modulated by EN2 was investigated in

321   two other cell lines. The mRNA expression level of SPARC was found to decrease by about 60%

322   in EN2-null TE-1 cells as determined by qRT-PCR. However, EN2 did not change the

323   expression of SPARC in EN2-Kyse150 cells when compared with its expression in NEO-

324   Kyse150 cells (Fig. S1E). These data demonstrate that EN2 is able to boost the expression of the

325   SPARC genes in Eca109 and TE-1 but not in Kyse150.

326   **The homeodomain is essential for the SPARC induction and the protumor function of EN2**

327   The sequence and structure of the homeodomain are highly conserved in the members of the

328   homeobox superfamily. The homeodomain of EN2 has a three-helix structure that directly

329   participates in DNA binding. Two mutants were created to evaluate the significance of the

330   homeodomain in the protumor function of EN2. The mutants each had a small deletion in the

331   homeodomain; the deletions were as follows: mut1 with a deletion of the residues from 283 to

332 292 and mut 2 with a deletion of the residues from 293 to 302 (Fig. 6A). The sequencing maps

333 around the mutated sites are shown in Fig. 6B. The expression vectors, each containing a

334 mutated EN2, were introduced respectively into Eca109 using the lentivirus system and

335 generating the Mut.1-Eca109 and Mut.2-Eca109 cell lines. The expression of the two mutant

336 transcripts of EN2 was verified using qRT-PCR (Fig. 6C). The effects of the two mutants were

337 evaluated for their ability to proliferate, migrate, and invade the cell line. Both mutants were

338 shown to hinder the promoting effects of EN2 on the proliferation of Eca109 (Fig. 6D). The

339 mutants largely eliminated the enhancing effects of EN2 on the cell's migratory abilities (Figs.

340 6E and 6F) and invasion in matrigel (Figs. 6G and 6H). The expression status of SPARC in the

341 Mut1-Eca109 and Mut2-Eca109 cell lines was investigated and the results revealed that the

342 mutations in the homeodomain also abrogate the function of EN2 in inducing the expression of

343 SPARC (Figs. 6I and 6J). Our results indicate that the homeodomain is essential for the protumor

344 effect of EN2.

345 **ShRNA-mediated knockdown of SPARC hampers the pro-oncogenic effect of EN2**

346 SPARC may be necessary for mediating the biological functions of EN2. We generated a shRNA

347 lentiviral vector specifically directed against the SPARC transcript to determine whether the

348 EN2-mediated tumor proliferation, migration, and invasion are dependent on SPARC expression.

349 A scramble sequence was used as the control. The introduction of the shRNA vector into NEO-

350 Eca109 and EN2-Eca109 successfully reduced the expression of SPARC proteins by 80% (Figs.

351 7A and 7B). Knockdown of SPARC significantly reduced the proliferation capacity of EN2-

352 Eca109 (Fig. 7C). We also observed the decreased capacities of the migration and invasion of the

353 shRNA-transfected cells (Figs. 7D-7G). This result demonstrates that SPARC plays a critical

354 role in mediating the biological function of EN2 in the Eca109 cell line.

355 **Discussion**

356 The poor prognosis and high mortality rates of esophageal cancer highlight the need to better

357 understand the molecular events leading to the progression of this disease. We demonstrated that

358 engrailed-2, a member of the homeobox superfamily, may be a potential biomarker in the

359 identification of the malignancy of ESCC and confirmed its oncogenic role in this cancer.

360 Certain members of the homeobox superfamily have been implicated in normal development as

361 well as in the pathological development of cancer. OCT-4 is a homeobox gene well known for its

362 function in generating induced pluripotent stem cells (Bhartiya, 2013; Seiler et al., 2011); this

363   gene has also been identified as an oncogene known for promoting the features of cancer stem

364   cells (Li et al., 2017; Phiboonchaiyanan & Chanvorachote, 2017). In addition to OCT-4, an

365   increasing body of evidence reveals that homeobox genes may participate in the promotion of

366   various malignant phenotypes such as the proliferation, migration, and invasion of cancers

367   (Hirao et al., 2019; Miwa & Kanda, 2019; Rodini et al., 2012; Song et al., 2019). We have

368   previously reported that HoxC6, another member of homeobox superfamily, functions as an

369   oncogene in ESCC (Tang et al. 2019). We therefore performed the correlation analysis using the

370   data retrieved from TCGA, and the result indicates that these two genes function independently

371   (Fig. S2). Nevertheless, these results suggest that HoxC6 and EN2 may complement each other

372   when using as the potential biomarkers in the diagnosis or treatment of ESCC. Additional

373   homeobox genes will likely be recognized as critical factors in the malignancy of ESCC, which

374   may provide clinical opportunities for the diagnosis and treatments of this cancer in the future.

375   EN2 functions as a transcription factor, much like other homeobox genes, binding directly to

376   specific DNA sites in the chromatin via the conserved homeodomain and controlling the

377   expression of downstream targets. In our experiment, EN2 was able to modulate the expressions

378   of hundreds of downstream targets. Although the expression of distinct sets of genes are affected

379   in various ESCC cell lines, it is likely that many of these genes are connected to the mailgnant

380   phenotype of cancer cells. For instance, the expression of SPARC is significantly upregulated

381   upon the expression of EN2 in two of three ESCC cell lines. We further demonstrated that

382   SPARC is capable of mediating the oncogenic effect of EN2 in the Eca109 cell lines. A similar

383   effect was not observed for EN2 on the expression of SPARC in Kyse150 cell lines; however,

384   there were many other oncogenic genes regulated upon the expression of EN2 in this cell line.

385   This phenomenon suggests that the mechanism underlying the biological function of EN2 may

386   be cell context-dependent. Our work confirms the importance of the homeodomain on the pro-

387   malignant effect of EN2 in ESCC cells. However, the homeodomain alone is not sufficient to

388   determine the DNA-binding specificity of a homeobox gene-encoded protein and the

389   involvement of the amino acid sequence outside of the homeodomain region is also required (van

390   Dijk & Murre, 1994; Peltenburg & Murre, 1997). The availability of other co-factors and the

391   accessibility of chromatin also influences the complexity of this system (Porcelli et al. 2019), and

392   may influence the outcome of EN2 expression in various cell lines. Further insight into the

393   molecular mechanisms will help to explain the biological effects of EN2 in ESCC.

394   The data presented in this work demonstrates that the biological effect of EN2 is correlated with

395   its role in transcription activation. Future studies should seek to clarify the structural basis and

396   components of EN2-containing transcription activation complexes.

397   **Conclusion**

398   We demonstrated that EN2 plays an oncogenic role in ESCC. Further, the biological function of

399   EN2 is mediated via the upregulation of downstream oncogenes. Our work provides more

400   information on the molecular mechanisms underlying the malignancy of this type of cancer. EN2

401   may serve as a potential candidate as a diagnostic marker or therapeutic target of ESCC in the

402   future.

403   **Acknowledgements**

404   We would like to thank our colleagues for their contribution to this study.

405   **References**

406   Bhartiya D. 2013. Are Mesenchymal Cells Indeed Pluripotent Stem Cells or Just Stromal Cells?
407   OCT-4 and VSELs Biology Has Led to Better Understanding. Stem Cells Int
408   2013:547501. 10.1155/2013/547501
409   Bose SK, Bullard RS, and Donald CD. 2008. Oncogenic role of engrailed-2 (en-2) in prostate cancer cell
410   growth and survival. *Transl Oncogenomics* 3:37-43.
411   Bressan RB, Dewari PS, Kalantzaki M, Gangoso E, Matjusaitis M, Garcia-Diaz C, Blin C, Grant V,
412   Bulstrode H, Gogolok S, Skarnes WC, and Pollard SM. 2017. Efficient CRISPR/Cas9-assisted
413   gene targeting enables rapid and precise genetic manipulation of mammalian neural stem cells.
414   *Development* 144:635-648. 10.1242/dev.140855
415   Carnesecchi J, Pinto PB, and Lohmann I. 2018. Hox transcription factors: an overview of multi-step
416   regulators of gene expression. *Int J Dev Biol* 62:723-732. 10.1387/ijdb.180294il
417   Chen J, Wang M, Xi B, Xue J, He D, Zhang J, and Zhao Y. 2012. SPARC is a key regulator of
418   proliferation, apoptosis and invasion in human ovarian cancer. PLoS One 7:e42413.
419   10.1371/journal.pone.0042413
420   Cong L, and Zhang F. 2015. Genome engineering using CRISPR-Cas9 system. *Methods Mol Biol*
421   1239:197-217. 10.1007/978-1-4939-1862-1_10
422   Domper Arnal MJ, Ferrandez Arenas A, and Lanas Arbeloa A. 2015. Esophageal cancer: Risk
423   factors, screening and endoscopic treatment in Western and Eastern countries. World J
424   Gastroenterol 21:7933-7943. 10.3748/wjg.v21.i26.7933
425   Fraenkel E, Rould MA, Chambers KA, and Pabo CO. 1998. Engrailed homeodomain-DNA complex at
426   2.2 A resolution: a detailed view of the interface and comparison with other engrailed structures.
427   *J Mol Biol* 284:351-361. 10.1006/jmbi.1998.2147
428   Friedrich J, Sorge S, Bujupi F, Eichenlaub MP, Schulz NG, Wittbrodt J, and Lohmann I. 2016.
429   Hox Function Is Required for the Development and Maintenance of the Drosophila
430   Feeding Motor Unit. Cell Rep 14:850-860. 10.1016/j.celrep.2015.12.077

431 Gujral TS, Chan M, Peshkin L, Sorger PK, Kirschner MW, and MacBeath G. 2014. A
432   noncanonical Frizzled2 pathway regulates epithelial-mesenchymal transition and
433   metastasis. Cell 159:844-856. 10.1016/j.cell.2014.10.032
434 Hirao N, Iwata T, Tanaka K, Nishio H, Nakamura M, Morisada T, Morii K, Maruyama N, Katoh
435   Y, Yaguchi T, Ohta S, Kukimoto I, Aoki D, and Kawakami Y. 2019. Transcription factor
436   homeobox D9 is involved in the malignant phenotype of cervical cancer through direct
437   binding to the human papillomavirus oncogene promoter. Gynecol Oncol 155:340-348.
438   10.1016/j.ygyno.2019.08.026
439 Hueber SD, and Lohmann I. 2008. Shaping segments: Hox gene function in the genomic age.
440   Bioessays 30:965-979. 10.1002/bies.20823
441 Hung JY, Yen MC, Jian SF, Wu CY, Chang WA, Liu KT, Hsu YL, Chong IW, and Kuo PL. 2017.
442   Secreted protein acidic and rich in cysteine (SPARC) induces cell migration and epithelial
443   mesenchymal transition through WNK1/snail in non-small cell lung cancer. *Oncotarget* 8:63691-
444   63702. 10.18632/oncotarget.19475
445 Kojima Y, Kondo Y, Fujishita T, Mishiro-Sato E, Kajino-Sakamoto R, Taketo MM, and Aoki
446   M. 2019. Stromal iodothyronine deiodinase 2 (DIO2) promotes the growth of intestinal
447   tumors in Apc(Delta716) mutant mice. Cancer Sci. 10.1111/cas.14100
448 Li L, Wei X, Wu B, Xiao Y, Yin M, and Yang Q. 2017. siRNA-mediated knockdown of ID1
449   disrupts Nanog- and Oct-4-mediated cancer stem cell-likeness and resistance to
450   chemotherapy in gastric cancer cells. Oncol Lett 13:3014-3024. 10.3892/ol.2017.5828
451 Lin Y, Totsuka Y, He Y, Kikuchi S, Qiao Y, Ueda J, Wei W, Inoue M, and Tanaka H. 2013.
452   Epidemiology of esophageal cancer in Japan and China. *J Epidemiol* 23:233-242.
453 Madissoon E, Jouhilahti EM, Vesterlund L, Tohonen V, Krjutskov K, Petropoulos S, Einarsdottir E,
454   Linnarsson S, Lanner F, Mansson R, Hovatta O, Burglin TR, Katayama S, and Kere J. 2016.
455   Characterization and target genes of nine human PRD-like homeobox domain genes expressed
456   exclusively in early embryos. *Sci Rep* 6:28995. 10.1038/srep28995
457 Mansour MA, and Senga T. 2017. HOXD8 exerts a tumor-suppressing role in colorectal cancer as an
458   apoptotic inducer. *Int J Biochem Cell Biol* 88:1-13. 10.1016/j.biocel.2017.04.011
459 Martin NL, Saba-El-Leil MK, Sadekova S, Meloche S, and Sauvageau G. 2005. EN2 is a candidate
460   oncogene in human breast cancer. *Oncogene* 24:6890-6901. 10.1038/sj.onc.1208840
461 McGrath SE, Michael A, Pandha H, and Morgan R. 2013. Engrailed homeobox transcription factors as
462   potential markers and targets in cancer. *FEBS Lett* 587:549-554. 10.1016/j.febslet.2013.01.054
463 Miwa T, and Kanda M. 2019. ASO Author Reflections: Homeobox C10 Influences on the
464   Malignant Phenotype of Gastric Cancer Cell Lines and its Elevated Expression Positively
465   Correlates with Recurrence and Poor Survival. Ann Surg Oncol. 10.1245/s10434-019-
466   07405-9
467 Morgan R. 2006. Engrailed: complexity and economy of a multi-functional transcription factor. *FEBS*
468   *Lett* 580:2531-2533. 10.1016/j.febslet.2006.04.053
469 Morgan R, Boxall A, Bhatt A, Bailey M, Hindley R, Langley S, Whitaker HC, Neal DE, Ismail
470   M, Whitaker H, Annels N, Michael A, and Pandha H. 2011. Engrailed-2 (EN2): a tumor
471   specific urinary biomarker for the early diagnosis of prostate cancer. Clin Cancer Res
472   17:1090-1098. 10.1158/1078-0432.CCR-10-2410
473 Morgan R, Bryan RT, Javed S, Launchbury F, Zeegers MP, Cheng KK, James ND, Wallace DM, Hurst
474   CD, Ward DG, Knowles MA, and Pandha H. 2013. Expression of Engrailed-2 (EN2) protein in
475   bladder cancer and its potential utility as a urinary diagnostic biomarker. *Eur J Cancer* 49:2214-
476   2222. 10.1016/j.ejca.2013.01.019
477 Pabo CO, and Sauer RT. 1992. Transcription factors: structural families and principles of DNA
478   recognition. *Annu Rev Biochem* 61:1053-1095. 10.1146/annurev.bi.61.070192.005201

479   Peltenburg LT, and Murre C. 1997. Specific residues in the Pbx homeodomain differentially
480   modulate the DNA-binding activity of Hox and Engrailed proteins. Development
481   124:1089-1098.
482   Phiboonchaiyanan PP, and Chanvorachote P. 2017. Suppression of a cancer stem-like phenotype
483   mediated by alpha-lipoic acid in human lung cancer cells through down-regulation of
484   beta-catenin and Oct-4. Cell Oncol (Dordr) 40:497-510. 10.1007/s13402-017-0339-3
485   Porcelli D, Fischer B, Russell S, and White R. 2019. Chromatin accessibility plays a key role in
486   selective targeting of Hox proteins. Genome Biol 20:115. 10.1186/s13059-019-1721-4
487   Ritchie ME, Phipson B, Wu D, Hu Y, Law CW, Shi W, and Smyth GK. 2015. limma powers
488   differential expression analyses for RNA-sequencing and microarray studies. Nucleic
489   Acids Res 43:e47. 10.1093/nar/gkv007
490   Rodini CO, Xavier FC, Paiva KB, De Souza Setubal Destro MF, Moyses RA, Michaluarte P,
491   Carvalho MB, Fukuyama EE, Head, Neck Genome Project G, Tajara EH, Okamoto OK,
492   and Nunes FD. 2012. Homeobox gene expression profile indicates HOXA5 as a
493   candidate prognostic marker in oral squamous cell carcinoma. Int J Oncol 40:1180-1188.
494   10.3892/ijo.2011.1321
495   Seiler K, Soroush Noghabi M, Karjalainen K, Hummel M, Melchers F, and Tsuneto M. 2011.
496   Induced pluripotent stem cells expressing elevated levels of sox-2, oct-4, and klf-4 are
497   severely reduced in their differentiation from mesodermal to hematopoietic progenitor
498   cells. Stem Cells Dev 20:1131-1142. 10.1089/scd.2010.0391
499   Shen ZY, Xu LY, Chen MH, Li EM, Li JT, Wu XY, and Zeng Y. 2003. Upregulated expression
500   of Ezrin and invasive phenotype in malignantly transformed esophageal epithelial cells.
501   World J Gastroenterol 9:1182-1186. 10.3748/wjg.v9.i6.1182
502   Song C, Han Y, Luo H, Qin Z, Chen Z, Liu Y, Lu S, Sun H, and Zhou C. 2019. HOXA10
503   induces BCL2 expression, inhibits apoptosis, and promotes cell proliferation in gastric
504   cancer. Cancer Med 8:5651-5661. 10.1002/cam4.2440
505   Tang L, Cao Y, Song X, Wang X, Li Y, Yu M, Li M, Liu X, Huang F, Chen F, and Wan H.
506   2019. HOXC6 promotes migration, invasion and proliferation of esophageal squamous
507   cell carcinoma cells via modulating expression of genes involved in malignant
508   phenotypes. PeerJ 7:e6607. 10.7717/peerj.6607
509   Teo WW, Merino VF, Cho S, Korangath P, Liang X, Wu RC, Neumann NM, Ewald AJ, and Sukumar S.
510   2016. HOXA5 determines cell fate transition and impedes tumor initiation and progression in
511   breast cancer through regulation of E-cadherin and CD24. *Oncogene* 35:5539-5551.
512   10.1038/onc.2016.95
513   Tian H, Li X, Jiang W, Lv C, Sun W, Huang C, and Chen R. 2016. High expression of AKR1C1
514   is associated with proliferation and migration of small-cell lung cancer cells. Lung
515   Cancer (Auckl) 7:53-61. 10.2147/LCTT.S90694
516   Toledo JR, Prieto Y, Oramas N, and Sanchez O. 2009. Polyethylenimine-based transfection method as a
517   simple and effective way to produce recombinant lentiviral vectors. *Appl Biochem Biotechnol*
518   157:538-544. 10.1007/s12010-008-8381-2
519   van Dijk MA, and Murre C. 1994. extradenticle raises the DNA binding specificity of homeotic
520   selector gene products. Cell 78:617-624.
521   Wan H, Li Y, Fan Y, Meng F, Chen C, and Zhou Q. 2012. A site-directed mutagenesis method
522   particularly useful for creating otherwise difficult-to-make mutants and alanine scanning.
523   Anal Biochem 420:163-170. 10.1016/j.ab.2011.09.019

524   Wu JI, Lin YP, Tseng CW, Chen HJ, and Wang LH. 2019. Crabp2 Promotes Metastasis of Lung
525   Cancer Cells via HuR and Integrin beta1/FAK/ERK Signaling. Sci Rep 9:845.
526   10.1038/s41598-018-37443-4
527   Yu G, Wang LG, Han Y, and He QY. 2012. clusterProfiler: an R package for comparing
528   biological themes among gene clusters. OMICS 16:284-287. 10.1089/omi.2011.0118
529   Zhang B, Li N, and Zhang H. 2018. Knockdown of Homeobox B5 (HOXB5) Inhibits Cell Proliferation,
530   Migration, and Invasion in Non-Small Cell Lung Cancer Cells Through Inactivation of the
531   Wnt/beta-Catenin Pathway. *Oncol Res* 26:37-44. 10.3727/096504017X14900530835262

532

Figure 1

Expression of EN2 is significantly elevated in ESCC.

(A, B) Microarray data retrieved from gene expression omnibus (GEO) repository were utilized to analyze EN2 expression at mRNA level in ESCC tissues including GSE130078 (normal=23, cancer=23) and GSE45670 (normal=10, cancer=28). (C) Data in TCGA database showed higher mRNA level of EN2 in ESCC tissues compared to adjacent normal tissues. (D) Expression of EN2 mRNA in 32 pairs of tumor samples and adjacent normal tissues as determined using qRT-PCR. (E) Representative images of IHC staining of EN2 in ESCC and adjacent normal tissues. (F) Expression of EN2 protein as determined by IHC(n=24). The IHC score of EN2 was calculated as the staining intensity (0, 1, 2, or 3) × positive percentage × 100.
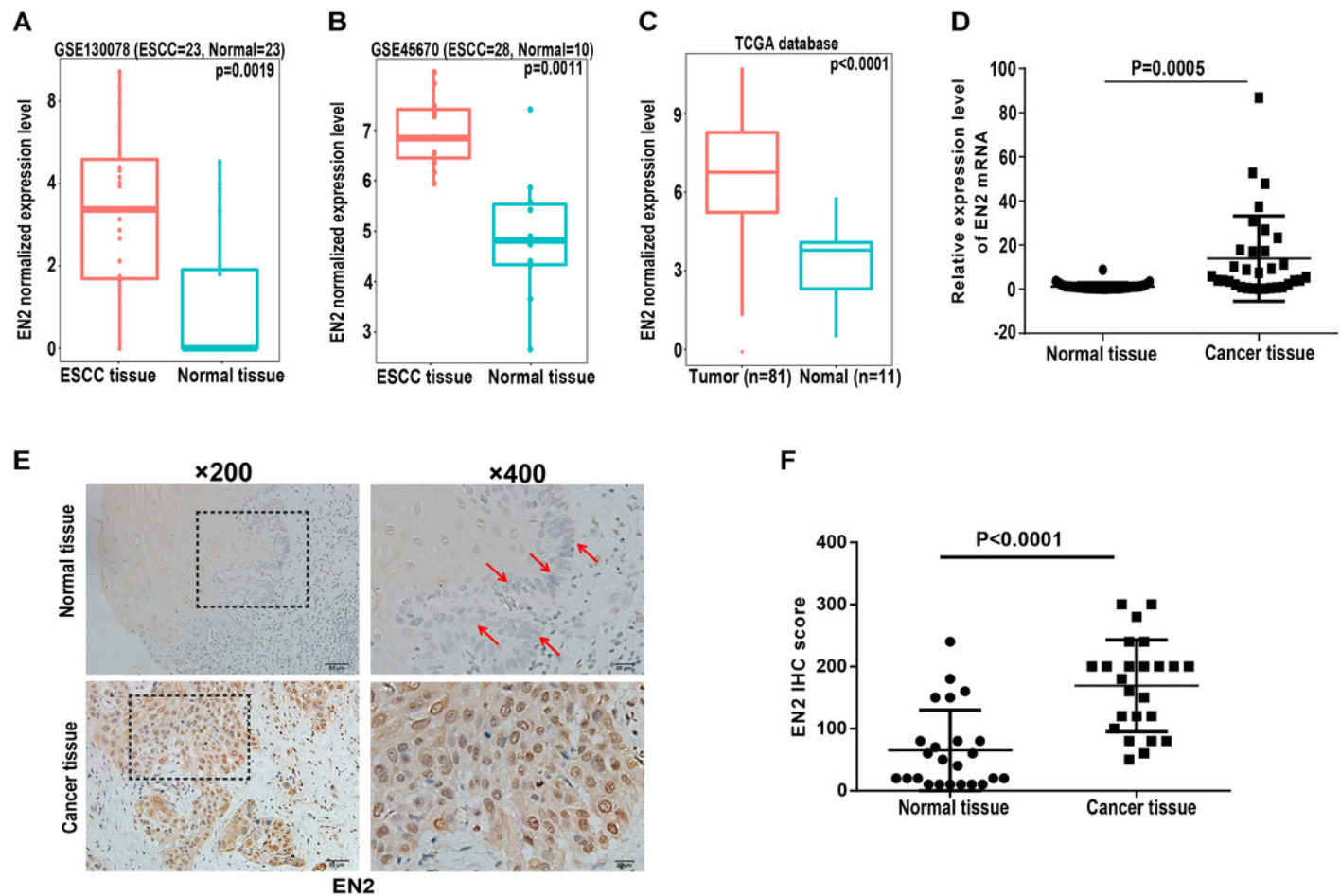
Figure 2

EN2 expression augments the growth and clonogenic abilities of ESCC cell lines.

(A) The mRNA expression of EN2 in three ESCC cell lines, in a mixture of total RNA extracted from normal esophageal samples adjacent to ESCC tumors of 32 patients, and in the SHEE control cell line was evaluated by means of qRT-PCR. (B) Eca109 and Kyse150 cells were infected with either EN2-containing or NEO-containing empty lentivirus particles. The mRNA expression level of EN2 was evaluated using qRT-PCR. (C, D) Fluorescent images of cancer cells stained with anti-EN2 antibody. EN2 staining is shown in green using FITC-labeled secondary antibody. Cell nuclei were stained blue (DAPI) and images were taken by confocal microscopy at ×20 magnification. (E) EN2 promoted cell growth as demonstrated by CCK-8 assay. (F) EN2 promoted cell growth as determined by the IncuCyteZOOM® live cell imaging assay. (G, H) Exogenous EN2 expression augmented the colony-forming ability of Kyse150 cell lines. (I, J) Exogenous EN2 expression augmented the colony-forming ability of Eca109 cell lines. (* $p < 0.05$, ** $p < 0.01$,*** $p < 0.001$).
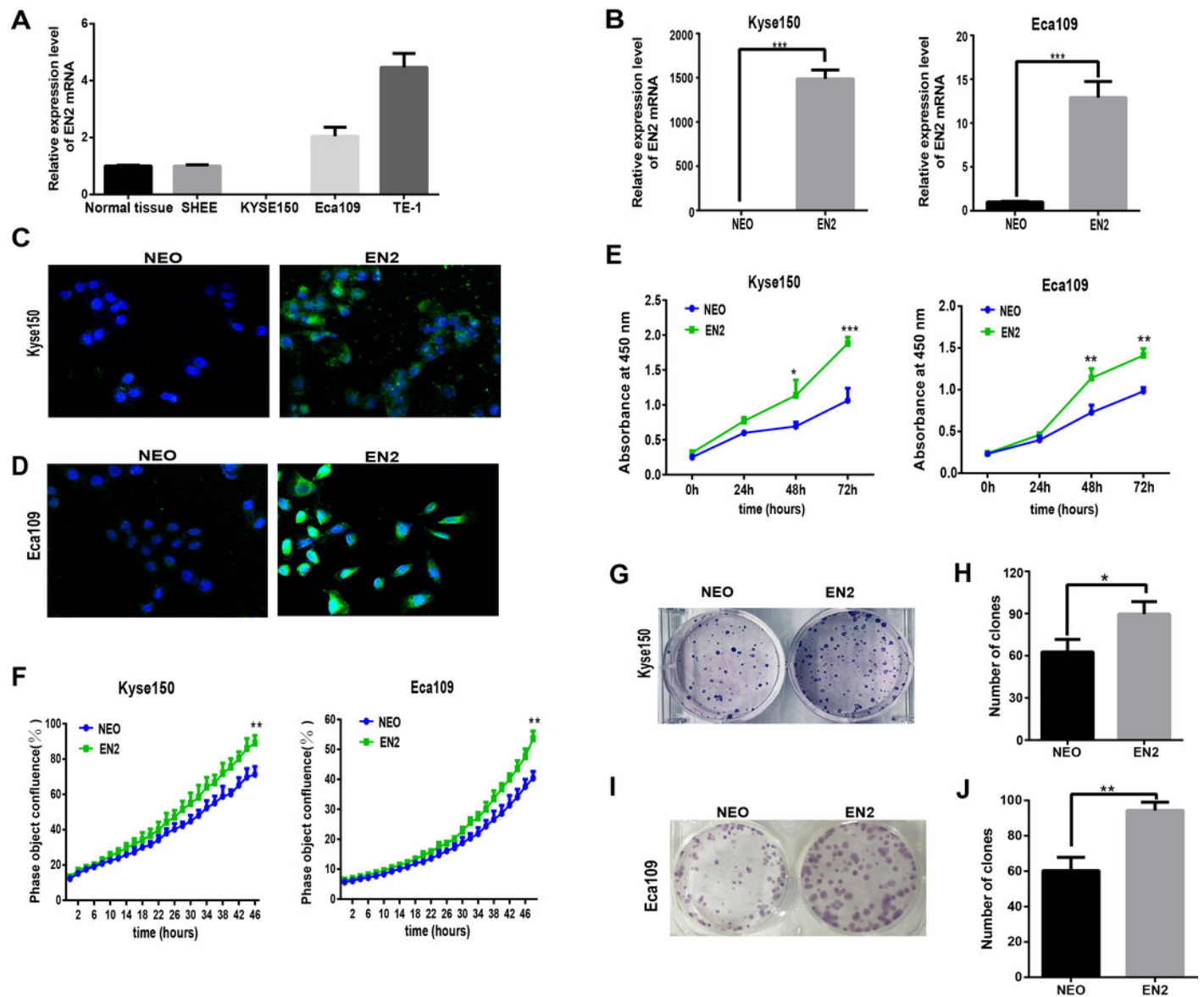
Figure 3

EN2 promotes the migration and invasion of ESCC cells.

(A, B) Migratory variation of Kyse150 cells expressing EN2 or NEO was evaluated using wound-healing assay. (C, D) Migratory variation of Eca109 cells expressing EN2 or NEO was evaluated using wound-healing assay. (E, F) Invasive variation of Kyse150 cells expressing EN2 or NEO was evaluated using Matrigel invasion assay. (G, H) Invasive variation of Eca109 cells expressing EN2 or NEO was evaluated using Matrigel invasion assay. Representative photographs (left) and quantification (right) are shown. The scale bars represent 300 μm. (** p < 0.01,*** p < 0.001).
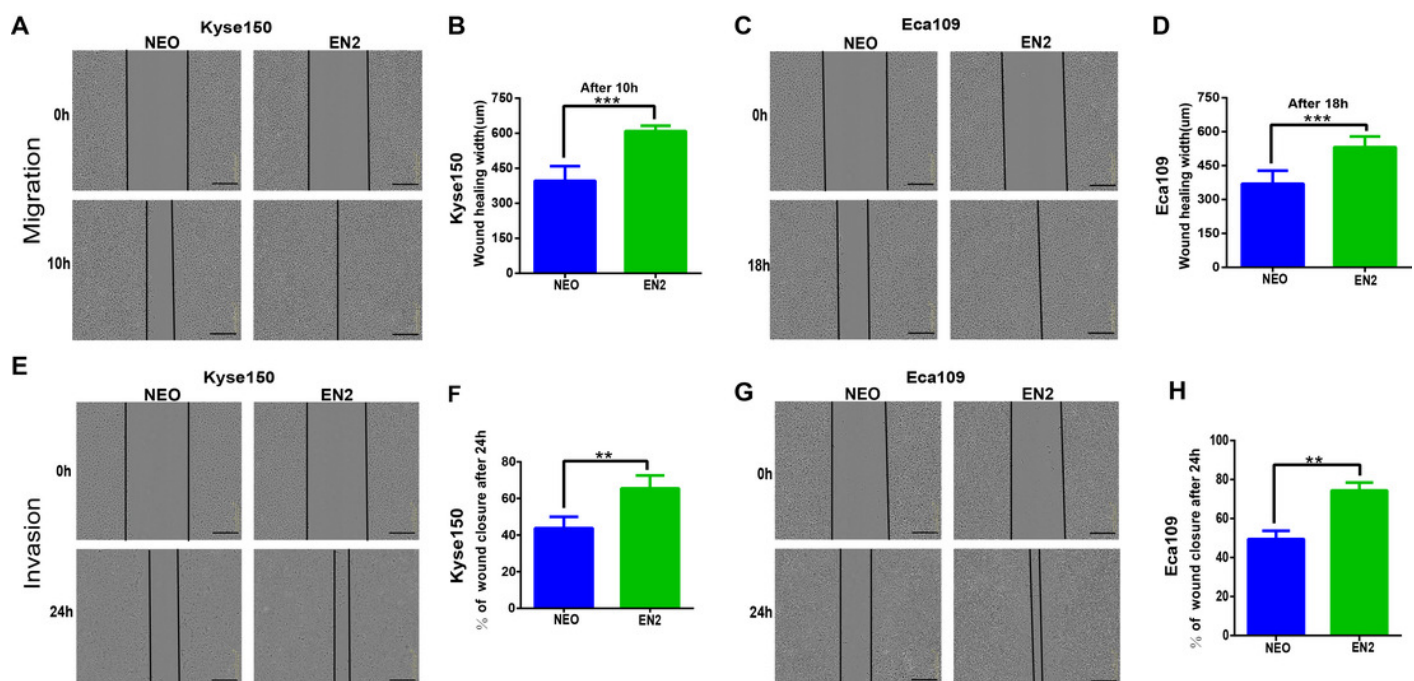
Figure 4

Silencing of EN2 negatively affects the proliferation, clonogenicity, migration, and invasion of TE-1 cells.

(A) Schematic representation of the CRISPR-Cas9 target site (marked in red), which is located at the first exon of the EN2 locus. The protospacer adjacent motif (PAM) is underlined. (B) The confirmation of effective disruption of the EN2 gene using the T7 endonuclease assay. The size of the T7 endonuclease I-digested DNA fragments is indicated on the right; lane M, 1, and 2 indicate the DNA marker (DL1000, Takara), the sample from the parental TE-1 cells transfected PX458 vector (control), and the sample from the EN2-disrupted cells. (C) The confirmation of effective disruption of EN2 protein using immunofluorescent staining. EN2 staining is shown in green (FITC-labeled secondary antibody). Cell nuclei are stained in blue (DAPI), images were taken by confocal microscopy at ×20 magnification. (D) Disruption of EN2 decreases cell growth as determined by the live-cell imaging assay. (E, F) Disruption of EN2 hampers the colony-forming ability of TE-1 cells. (G, H) Disruption of EN2 suppresses the migratory potential of TE-1 cells. (I, J) Disruption of EN2 suppresses the invasive capacity of TE-1 cells. The scale bars equal 300 μm. (* $p < 0.05$, *** $p < 0.001$).

A

Knockout of EN2 using CRISPR/CAS9 system

Exon1   Exon2

Target site   PAM
CGGCGG CGGTAGCAGCCCGGGCGAAG CGG ACACCGGGCGCCGGCGG

B

M   1   2
1000 —   ← 1098bp
700 —   ← 744bp
400 —
300 —   ← 354bp
200 —
100 —

C

Negative control   TE1/Cas9-Con   TE1/Cas9-EN2

D

Phase object confluence(%)

— TE1/Cas9-Con
— TE1/Cas9-EN2

***

time(hours)

E

TE1/Cas9-Con   TE1/Cas9-EN2

F

Number of clones

*

TE1/Cas9-Con   TE1/Cas9-EN2

G

TE1/Cas9-Con   TE1/Cas9-EN2

Migration

0h

24h

H

Wound healing width(um)

After 24h
***

TE1/Cas9-Con   TE1/Cas9-EN2

I

TE1/Cas9-Con   TE1/Cas9-EN2

Invasion

0h

24h

J

% of wound closure after 24h

***

TE1/Cas9-Con   TE1/Cas9-EN2

Figure 5

EN2 upregulates the expression of SPARC.

(A) Volcano maps show the differentially expressed genes in EN2-Eca109 as compared with the NEO-Eca109 cells. (B) Gene ontology (GO) analysis identified biological processes impacted by EN2 upregulated genes in Eca109 cells. (C) Gene ontology (GO) analysis identified biological processes impacted by EN2 downregulated genes in Eca109 cells. (D) Expression of the upregulated genes with high fold-change in EN2-Eca109 and NEO-Eca109 cells by means of qRT-PCR. (E) Examination of SPARC protein in EN2-Eca109 and NEO-Eca109 cells using the western blot assay. (F) Correlation analysis of EN2 and SPARC expression in ESCC tissue samples (n = 32).
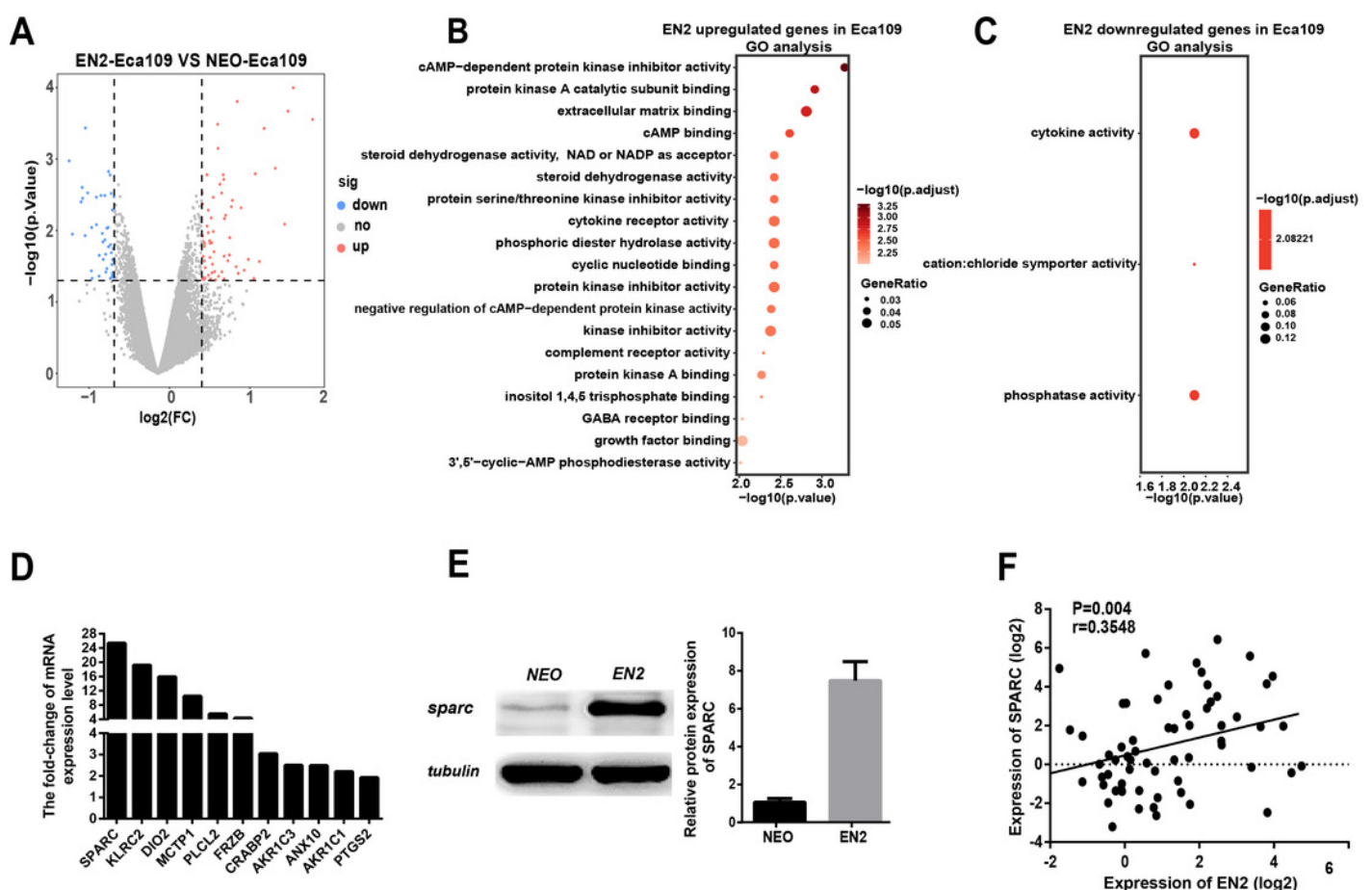
Figure 6

The homeodomain is essential for the SPARC induction and the protumor function of EN2.

(A) Schematic map of the two EN2 mutants with small deletions in the homeodomain region. α1, α2, and α3 indicate the three-helix structure in the homeodomain. (B) Confirmation of the expected mutations using the Sanger sequencing assay. The red triangles indicate the positions where part of the sequences are deleted. (C) The mRNA expressions of the EN2 and mutants were analyzed by qRT-PCR in Eca109 cells. EN2, Mut.1, and Mut.2 indicate the Eca109 cells infected with wild-type EN2, mutant 1, and mutant 2 expression lentivirus, respectively. (D) Analysis of the effect of the two mutants of EN2 on cell proliferation. (E, F) Analysis of the effect of the two mutants of EN2 on cell migration. (G, H) Analysis of the effect of the two mutants of EN2 on cell invasion. The scale bars represent 300 μm. (I, J) The mutations in the homeodomain attenuate the SPARC-inducing ability of the wild-type EN2 as determined by western blot assay. (* $p < 0.05$; ** $p < 0.01$).
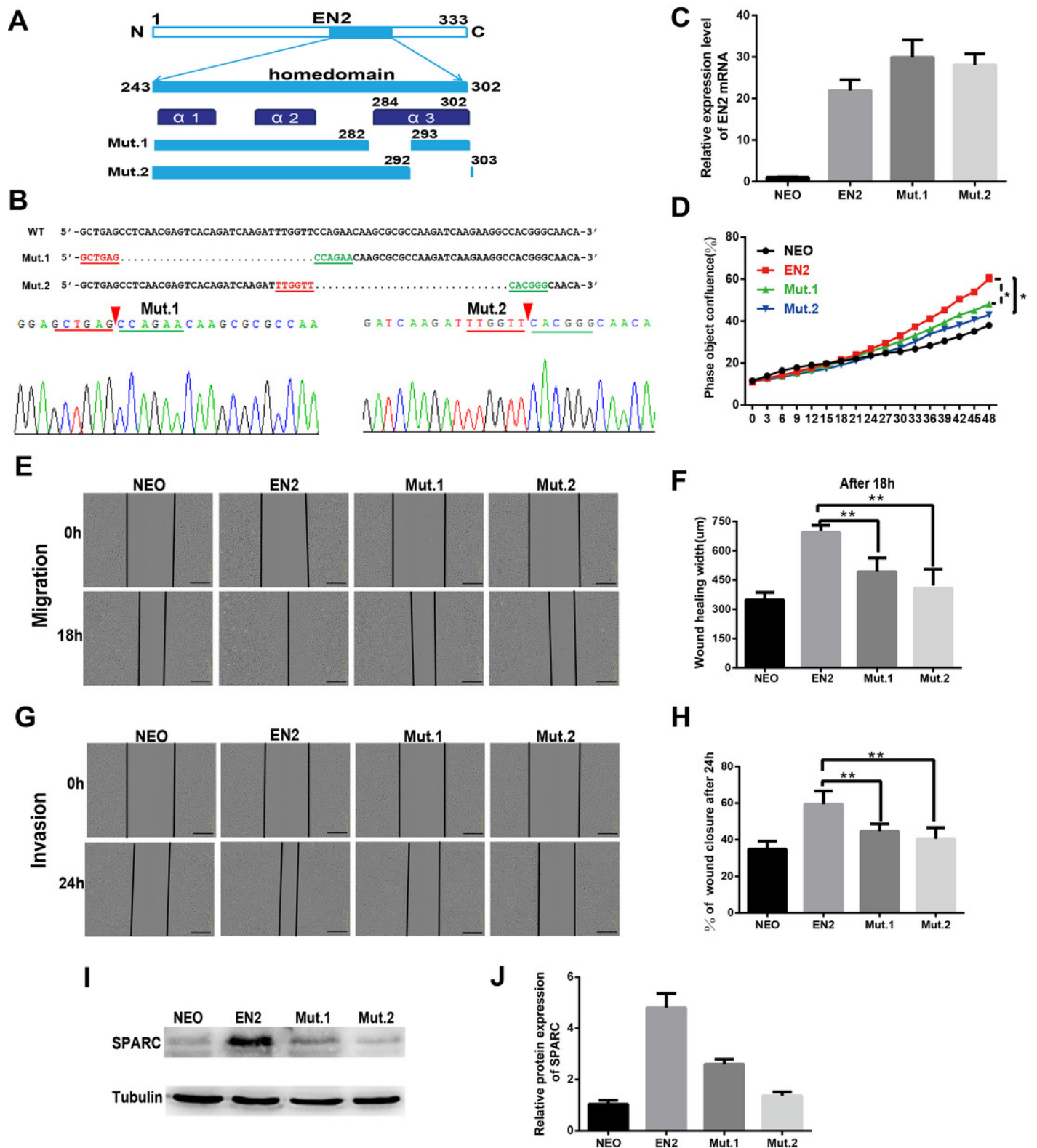
Figure 7

ShRNA-mediated knockdown of SPARC hampers the pro-oncogenic effect of EN2.

(A, B) Analysis of the efficiency of SPARC knockdown in EN2-Eca109 cells by means of the western blot assay. (C) The effect of SPARC knockdown on EN2-induced cell proliferation as determined by the live-cell imaging assay. (D, E) The effect of SPARC knockdown on EN2-induced cell motility as determined by the wound healing assay. (F, G) The effect of SPARC knockdown on EN2-induced cell invasion as determined by the Matrigel invasion assay. The scale bars represent 300 μm. (** $p < 0.01$).